



1 ***Fifty-six years of Surface Solar Radiation and Sunshine***
2 ***Duration at the Surface in São Paulo, Brazil: 1961 - 2016***

3

4 ***Marcia Akemi Yamasoe¹, Nilton Manuel Évora do Rosário²,***
5 ***Samantha Novaes Santos Martins Almeida³, Martin Wild⁴***

6 [1] Departamento de Ciências Atmosféricas, Instituto de Astronomia, Geofísica e
7 Ciências Atmosféricas, Universidade de São Paulo, São Paulo, Brazil

8 [2] Departamento de Ciências Ambientais, Universidade Federal de São Paulo,
9 Diadema, São Paulo, Brazil

10 [3] Seção de Serviços Meteorológicos do Instituto de Astronomia, Geofísica e Ciências
11 Atmosféricas, Universidade de São Paulo, São Paulo, Brazil

12 [4] Institute for Atmospheric and Climate Science, ETH Zurich, Switzerland

13

14 Correspondence to: M. A. Yamasoe (marcia.yamasoe@iag.usp.br)

15



Long-Term Analysis of Surface Solar Radiation 2

16

17

Abstract

18 Fifty-six years (1961 – 2016) of daily surface downward solar irradiation,
19 sunshine duration, diurnal temperature range and the fraction of the sky covered by
20 clouds in the city of São Paulo, Brazil, were analyzed. The main purpose was to
21 contribute to the characterization and understanding of the dimming and brightening
22 effects on solar global radiation in this part of South America. As observed in most of
23 the previous studies worldwide, in this study, during the period between 1961 up to the
24 early 1980's, more specifically up to 1983, a negative trend in surface solar irradiation
25 was detected in São Paulo, characterizing the occurrence of a dimming effect. A similar
26 behavior, a negative trend, was also observed for sunshine duration and the diurnal
27 temperature range, the three variables in opposition to the trend in the sky cover
28 fraction. However, a brightening effect, as observed in western industrialized countries
29 in more recent years, was not observed. Instead, for surface downward irradiation, the
30 negative trend persisted and still in consonance to the cloud cover fraction increasing
31 trend. The trends for sunshine duration and the diurnal temperature range, by contrast,
32 changed signal. Some possible causes for the discrepancy were discussed, such as the
33 frequency of fog occurrence, urban heat island effects, aerosol changes and greenhouse
34 gas concentration increase. Future studies on aerosol effect are encouraged, particularly
35 with higher temporal resolution as well as modeling studies, to better analyze the
36 contribution of each possible causes.

37



38 **1 Introduction**

39 Ultimately, the downward solar radiation at the surface is the main source of
40 energy that drives Earth's biological, chemical and physical processes (Wild et al.,
41 2013, Kren et al., 2017), from local to global scales. Therefore, the assessment of the
42 variability of the downward solar radiation at the surface is a key step in the efforts to
43 understand Earth's climate system variability. Before reaching the surface, solar
44 radiation can be attenuated mainly by aerosols and clouds, through scattering and
45 absorption processes, and to a lesser extent, through Rayleigh scattering by atmospheric
46 gases, absorption by ozone and water vapor, for example. In this context, during the last
47 half-century, long term changes in the amount of surface solar radiation (SSR) have
48 been investigated worldwide (Dutton et al., 1991, Stanhill and Cohen 2001, Wild et al.
49 2005, Shi et al., 2008, Wild, 2009, 2012, Ohvri, et al., 2009). At least two trends have
50 been well established and documented, a decline in surface solar radiation between
51 1950s and 1980s, named "Global Dimming" and an increase, from 1980s to 2000s,
52 termed "Brightening" (Stanhill and Cohen, 2001; Wild, 2009, 2012).

53 The global dimming definition, according to Stanhill and Cohen (2001), refers to
54 a widespread and significant reduction in global irradiance, that is the flux of solar
55 radiation reaching the earth's surface both in the direct solar beam and in the diffuse
56 radiation scattered by the sky and clouds. However, among these studies, while the
57 dimming phase has been a consensus for all locations analyzed, the brightening phase
58 was not (Wild, 2012). Over India, for example, the dimming phase seems to last
59 throughout the 2000s (Kumari and Goswami, 2010). The continuous dimming in India
60 and the renewed dimming in China from 2000s, opposing to a persistent brightening
61 over Europe and the United States, have been linked to trends in atmospheric
62 anthropogenic aerosol loadings (Wild, 2012). By contrast, other studies suggested that



Long-Term Analysis of Surface Solar Radiation 4

63 changes in cloud cover rather than anthropogenic aerosol emissions played a major role
64 in determining solar dimming and brightening during the last half century (Stanhill et
65 al., 2014). Therefore, the drivers of dimming and brightening are a matter of ongoing
66 research and debate. The role of these trends in the masking of temperature increase due
67 to the greenhouse gases (GHG) has been discussed (Wild et al., 2007). Furthermore, a
68 comprehensive assessment of the spatial scale of both dimming and brightening is
69 critical for a conclusive analysis of the likely drivers and implications for the current
70 global climate variability. Large portions of the globe are still lacking any evaluation on
71 this matter, such as Africa (Wild, 2009), which is a challenge for the spatial
72 characterization of both dimming and brightening trends.

73 Among the rare studies focusing on the South American subcontinent, Raichijk
74 (2012) discussed the trends over South America, analyzing sunshine duration (SD) data
75 from 1961 to 2004. The author divided South America in five climatic regions. In three
76 of them, also the one where the city of São Paulo is located, statistically significant
77 negative trends were observed on an annual basis, from 1961 up to 1990. From 1991 to
78 2004 a positive trend was observed in four of the five regions with a significance level
79 higher than 90%.

80 The alternative use of SD is mainly due to the lack of a consistent long-term
81 network for the monitoring of SSR across the continent, therefore alternative proxies
82 have to be found in order to provide an estimate of SSR long term trends. Another
83 variable commonly used to investigate SSR trends is the diurnal temperature range
84 (DTR), the difference between daily maximum (T_{\max}) and minimum (T_{\min}) air
85 temperature measured near the surface (Bristow and Campbell, 1984, Wild et al. 2007,
86 Makowski et al. 2008).



Long-Term Analysis of Surface Solar Radiation 5

87 The present study takes advantage of fifty-six years of a unique high quality
88 concurrent records of surface solar irradiation (SSR), sunshine duration (SD), diurnal
89 temperature range (DTR) and sky cover fraction (SCF), i.e., the fraction of the sky
90 covered by clouds, from 1961 to 2016, in the city of São Paulo, Brazil, to provide a
91 perspective on dimming and brightening trends with an extended database.

92 Thus, we propose to answer two questions in this study: 1) How was the decadal
93 variability of SSR over the 56 years of data?; 2) Can SD and DTR be adopted as proxies
94 to infer SSR variability in São Paulo? To answer to these questions, we organize the
95 manuscript as follows: in part 2 we present the data and methods of analysis; section 3
96 is divided in 3 parts. In the first part we discuss the annual trends in SSR, SD and DTR;
97 in the second, we focus the analysis on cloud free days; in the third part of section 3 we
98 discuss the trends in the maximum and minimum air temperatures near the surface.
99 Section 4 summarizes the main conclusions and discusses possible future work on the
100 subject.

101

102 **2 Observational Data and Methods**

103 The long term measurements used in this study were collected at the
104 meteorological station operated by the Instituto de Astronomia, Geofísica e Ciências
105 Atmosféricas from the Universidade de São Paulo (IAG/USP), located at latitude
106 23.65° S and longitude 46.62° W, 799 m above sea level. Figure 1 shows the
107 geographical location of the meteorological station. The site is surrounded by a
108 vegetated area due to its location inside a park.

109



Long-Term Analysis of Surface Solar Radiation 6



110

111 Figure 1 – São Paulo state and a zooming in view of São Paulo Metropolitan Area and
112 the location of the meteorological station of Instituto de Astronomia, Geofísica e
113 Ciências Atmosféricas from Universidade de São Paulo (EM-IAG). Adapted from ©
114 Google Earth (US Dept. of State Geographer – Data SIO, NOAA, U. S. Navy, NGA,
115 GEBCO - Image Landsat/Copernicus).

116

117 The downward solar irradiation has been measured since 1961 using an
118 *Actinograph Fuess model 58d*, with 5% uncertainty (Plana-Fattori and Ceballos, 1988).
119 Sunshine duration data was collected with a Campbell-Stokes sunshine recorder
120 (Horseman et al., 2008) from 1933 to the present, while daily maximum and minimum
121 air temperatures started to be monitored in 1935. Daily maximum and minimum
122 temperatures were used to estimate the diurnal temperature range as it is simply the
123 difference between the maximum and minimum daily temperatures. Diurnal sky cover
124 fraction was determined from visual inspection made every hour from 7:00 AM to
125 6:00 PM (local time) (Yamasoe et al. 2017).

126 Annual mean values of downward solar irradiation data at the surface were used
127 to characterize dimming and brightening trends while sunshine duration and diurnal
128 temperature range measurements at the same site were used to provide independent
129 information.

130 In order to detect possible temporal changes, avoiding autocorrelation in the
131 data, the modified Mann-Kendall trend test proposed by Hamed and Rao (1998) was
132 applied to the variables, while the regression coefficient was estimated based on Sen



Long-Term Analysis of Surface Solar Radiation 7

133 (1968). A statistically significant trend at the 95% confidence level was detected if the
134 absolute value of Z was above 1.96.

135 According to the meteorological station records, completely cloud free days are
136 extremely rare in São Paulo, being more common from June to the beginning of
137 September, corresponding to the southern hemisphere winter time, when dry conditions
138 prevail in the region (Yamasoe et al., 2017). The number of days without clouds per
139 year, from sunrise to sunset, varied from 1 to 23. Also, the impact of aerosol in SSR is
140 higher from August to October, when advection of smoke plume from long range
141 transport can reach São Paulo, summing up to the local pollution. Thus, in order to
142 analyze how clear sky conditions varied during the last 56 years, we restricted the data
143 to the months of July to October, to minimize the effect of any possible seasonal drift in
144 the aerosol characteristics throughout the years. Following Manara et al. (2016), days
145 with SCF of up to 0.1 were allowed, in order to increase the number of clear days per
146 year. Thus, only years with 9 or more days, in the specified months, were included in
147 the study.

148 For the analysis, atmospheric transmittance was estimated dividing the measured
149 daily surface irradiation (SSR) by the expected irradiation at the top of the atmosphere
150 (TSR). Daily measured sunshine duration (SD or n) was also normalized to the day-
151 length (N). Top of the atmosphere irradiation and day length were estimated using
152 formulas proposed by Paltridge and Platt (1976). Observers at the meteorological
153 station also take note on the occurrence of fog every day. If fog was observed, the day
154 received the number 1, otherwise, the number is 0. For each clear sky day, information
155 on fog observation was verified. The fraction of cloud free days with foggy conditions
156 for each year was then estimated for the months of July to October, to verify any
157 possible influence on SSR and SD. Moreover, since horizontal visibility information is



Long-Term Analysis of Surface Solar Radiation 8

158 also registered at the same time as the sky cover fraction, we included this information
159 in this analysis as well. Table 1 presents the registered code for horizontal visibility and
160 the corresponding distance range. Horizontal visibility can also be affected by haze and
161 fog conditions but is less sensitive to cloud variability.

162

163 Table 1 – Adopted codes for visibility records at the meteorological station and
164 corresponding distance ranges.

Code	Distance (meter)
0	Less than 50
1	50 to 200
2	200 to 500
3	500 to 1000
4	1000 to 2000
5	2000 to 4000
6	4000 to 10000
7	10000 to 20000
8	20000 to 50000
9	> 50000

165

166

167

168 To complement the analysis, aerosol columnar loading information from satellite
169 products such as the Absorbing Aerosol Index (AAI) from multi-sensor retrievals
170 (TOMS, GOME-1, SCIAMACHY, OMI, GOME-2A and GOME-2B) (Herman et al.,
171 1997, Torres et al., 1998, Graaf et al., 2005, Tilstra et al., 2014) and aerosol optical
172 depth (AOD) from MODIS (Moderate Resolution Imaging Spectroradiometer) onboard
173 Terra and Aqua satellites (Kaufman et al., 1997) were included. Shortly, the Absorbing
174 Aerosol Index indicates the presence of aerosol particles in the atmosphere with high
175 absorption efficiency in the ultraviolet spectrum. The product analyzed is the annual



Long-Term Analysis of Surface Solar Radiation 9

176 mean value with a spatial resolution of 1° by 1° in a box from 47° W to 46° W and 24° S
177 to 23° S which includes São Paulo Metropolitan Area, for the months of July to
178 October, from 1979 up to 2016 (<http://www.temis.nl/airpollution/absaai/>). The AOD
179 product is a combination of the Dark Target (Kaufman et al., 1997, Remer et al., 2005)
180 and the Deep Blue (Hsu et al., 2014) retrieval algorithms also degraded to the spatial
181 resolution of 1° by 1° , averaged annually from 2000 (for Terra) and 2002 (for Aqua) to
182 2016, also considering only the dry season months obtained from the NASA Giovanni
183 dataset site (<https://giovanni.gsfc.nasa.gov/giovanni/>).

184

185 **3 Results**

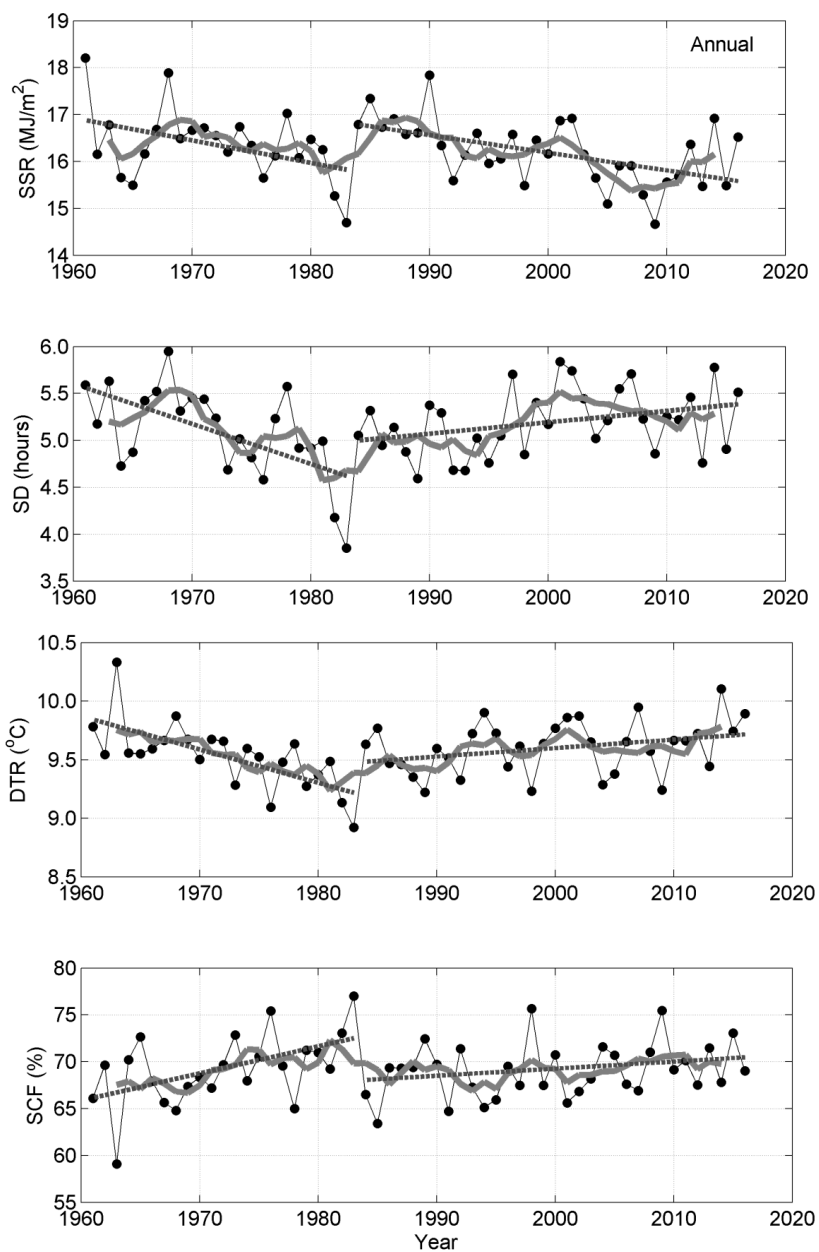
186 **3.1 SSR, SD, DTR and SCF annual mean variability and trends**

187 Figure 2 illustrates the time series of the annual mean values for SSR, SD, DTR
188 and SCF, showing that all the analyzed variables exhibited a large variability from year
189 to year. SSR, SD and DTR presented a decaying trend up to the beginning of the
190 1980's, in opposition, therefore consistent, to the SCF trend. According to Rosas et al.
191 (2019), who analyzed the same cloud fraction database from the meteorological station,
192 focusing on the climatology for different cloud types and base heights, all cloud types,
193 except for middle level clouds, presented a positive trend, which is confirmed by this
194 study. A statistically significant trend, at the 95% level, was observed for stratiform
195 cloud fraction of 4.8 % per decade and for cirrus of 1.4 % per decade, from 1958 to
196 1988.

197



Long-Term Analysis of Surface Solar Radiation 10



198

199

200 Figure 2 – Annual mean variability of surface solar irradiation (SSR), sunshine duration
201 (SD), diurnal temperature range (DTR) and sky cover fraction (SCF). Gray curves
202 represent 5 years moving averages and dotted lines are the result of trend analysis from
203 1961 to 1983 and from 1984 to 2016.

204



Long-Term Analysis of Surface Solar Radiation 11

205 Returning to Figure 2, the gray curve represents the 5 years moving average,
206 while the dotted line indicates the result of the modified Mann-Kendall trend analysis,
207 discussed ahead. The year of 1983 was the one presenting the lowest annual mean value
208 for SSR, SD and DTR, clearly as a response to the peak of SCF observed in that year,
209 which is worth to mention, was characterized by a strong El Niño event. According to
210 the Earth System Research Laboratory from the National Oceanic and Atmospheric
211 Administration (ESRL/NOAA), it is listed amongst the 24 strongest El Niño events and
212 lasted from April 1982 up to September 1983
213 (<https://www.esrl.noaa.gov/psd/enso/climaterisks/years/top24enso.html>). This 1983 El
214 Niño effect was also detected in rainfall data over the São Paulo Metropolitan Area
215 (Obregón et al., 2014), although the authors claim that such influence, at least on
216 rainfall variability, is detectable but is multifaceted and depends on the life cycle of
217 each ENSO event. Xavier et al. (1995), trying to identify a possible influence of ENSO
218 on precipitation extremes in the month of May, classified both May 1983 and May 1987
219 as exceptional extremes of precipitation. Their conclusion was that strong El Niño
220 events can affect the spatial organization of rainfall around São Paulo city. A more
221 recent study performed by Coelho et al. (2017), using daily precipitation data from 1934
222 to 2013 from the same meteorological station analyzed in this research, concluded that
223 El Niño conditions in July tend to increase precipitation in the following spring, also
224 anticipating the onset of the rainy season. No study was found about the possible effect
225 of ENSO on cloud cover over São Paulo. According to Rosas et al. (2019), middle and
226 high level clouds presented high positive anomalous cloud amount in 1983.

227 After 1983, the trend behavior of all variables changed, what motivated us to
228 separate the time series analysis in two periods, the first from 1961 to 1983 and the
229 second from 1984 up to 2016. The results of the modified Mann-Kendall trend test for



Long-Term Analysis of Surface Solar Radiation 12

230 each period are presented in Table 2, considering both annual and seasonal variabilities.
 231 Bold values indicate trends that are statistically significant at the 95% confidence level.
 232 From the table, in the first period, SSR, SD and DTR presented a decreasing trend,
 233 while SCF a positive one, increasing at a rate of 2.9% per decade. Except for SSR, all
 234 trends were statistically significant, with daily SD decreasing at a rate of 0.37 hours per
 235 decade and the diurnal temperature range declining at a rate of 0.49°C per decade.
 236 Looking at the seasonal variability, southern hemisphere autumn (MAM) and winter
 237 (JJA) presented statistically significant decreasing trends for SSR, SD and DTR.
 238 Springtime (SON) presented statistically significant decreasing trends also for SD and
 239 DTR. For SCF, statistically significant positive trends were observed for JJA and SON
 240 only.

241

242 Table 2 - Modified Mann-Kendall trend test results for P eriod 1, from 1961 to 1983,
 243 and P eriod 2, from 1984 to 2016, considering each season and in an annual basis for
 244 the surface solar radiation (SSR), sunshine duration (SD), diurnal temperature range
 245 (DTR) and sky cover fraction (SCF). The trend was estimated as the slope of the linear
 246 fit between the variable of interest and year.

SSR						
	Period 1: 1961-1983			Period 2: 1984-2016		
Time interval	Trend ^a	Z	p	Trend ^a	Z	P
Annual	-0.42	-1.74	0.081	-0.41	-3.18	0.001
DJF	-0.66	-1.11	0.267	-0.54	-2.62	0.009
MAM	-0.78	-2.48	0.013	-0.26	-1.72	0.085
JJA	-0.48	-1.98	0.048	-0.18	-1.97	0.049
SON	-0.25	-0.96	0.335	-0.58	-2.46	0.014

SD						
	Period 1: 1961-1983			Period 2: 1984-2016		



Long-Term Analysis of Surface Solar Radiation 13

Time interval	Trend ^b	Z	p	Trend ^b	Z	P
Annual	-0.37	-3.41	0.001	0.11	2.13	0.033
DJF	-0.41	-1.06	0.291	-0.01	-0.12	0.905
MAM	-0.53	-2.27	0.023	0.22	1.61	0.107
JJA	-0.54	-3.38	0.001	0.20	2.06	0.039
SON	-0.47	-2.31	0.021	0.03	0.20	0.840

DTR						
Period 1: 1961-1983				Period 2: 1984-2016		
Time interval	Trend ^c	Z	p	Trend ^c	Z	P
Annual	-0.49	-3.33	0.001	0.16	1.84	0.065
DJF	-0.32	-1.61	0.107	0.15	1.72	0.085
MAM	-0.58	-2.54	0.011	0.16	1.53	0.125
JJA	-0.61	-2.91	0.004	0.14	1.38	0.171
SON	-0.58	-2.64	0.008	0.02	0.17	0.865

SCF						
Period 1: 1961-1983				Period 2: 1984-2016		
Time interval	Trend ^d	Z	p	Trend ^d	Z	P
Annual	2.9	2.48	0.013	0.8	1.78	0.075
DJF	0.5	0.42	0.673	0.3	0.38	0.700
MAM	2.9	1.58	0.113	0.6	0.76	0.448
JJA	3.5	2.54	0.011	0.8	0.57	0.566
SON	3.8	2.12	0.034	1.5	1.22	0.221

247 Units of trend: a) kJ m^{-2} per decade; b) hours per decade; c) $^{\circ}\text{C}$ per decade; d)

248 % per decade

249

250

251



Long-Term Analysis of Surface Solar Radiation 14

252 In the first period, SSR and its proxies presented trends consistent with SFC
253 features, i.e., as SFC increased over time, the others decreased. In the second period,
254 from 1984 to 2016, this behavior combination changed. While SSR still presented, on
255 an annual basis, a statistically significant decreasing trend, of -0.41 kJm^{-2} per decade,
256 SD and DTR trends changed from negative to positive, being statistically significant
257 only for SD, with a trend of 0.11 hours per decade. SFC continued to present a positive
258 trend, but not statistically significant. It is worth noting that, even though the trends are
259 not statistically significant, the pattern between SSR and SFC observed in the first
260 period remained in the second, and in all seasons. According to Rosas et al. (2019),
261 statistically significant trends, positive for low clouds (3.2% per decade) and negative
262 for mid level clouds (-5.5% per decade), were observed in the last 30 years, from 1987
263 to 2016. Such analysis indicated that changes in cloud types also influenced the
264 variability of SSR and proxies. However, other factors, rather than only cloud changes,
265 were also responsible for the variability of SD and DTR, as analyzed in the next
266 sections.

267 **3.2 Analysis of cloud free days**

268 From the good correlation between SSR and SFC, and based on previous results
269 from Yamasoe et al. (2017), cloud cover seems to be the main driver of SSR attenuation
270 in São Paulo. To evaluate the solely contribution of aerosol direct effect, we relied on a
271 limited number of completely clear sky days since the current study was based on
272 irradiation data, i.e., integrated from sunrise to sunset. However, in order to have a clue
273 on its effect, mean atmospheric transmittance was estimated, during cloud free
274 conditions, i.e., considering only days with SCF less than 0.1 and with, at least, 9 cloud
275 free days per year. Most of those days were observed in winter and beginning of spring,
276 when dry conditions prevail, aerosol loading related to local sources is higher and when



Long-Term Analysis of Surface Solar Radiation 15

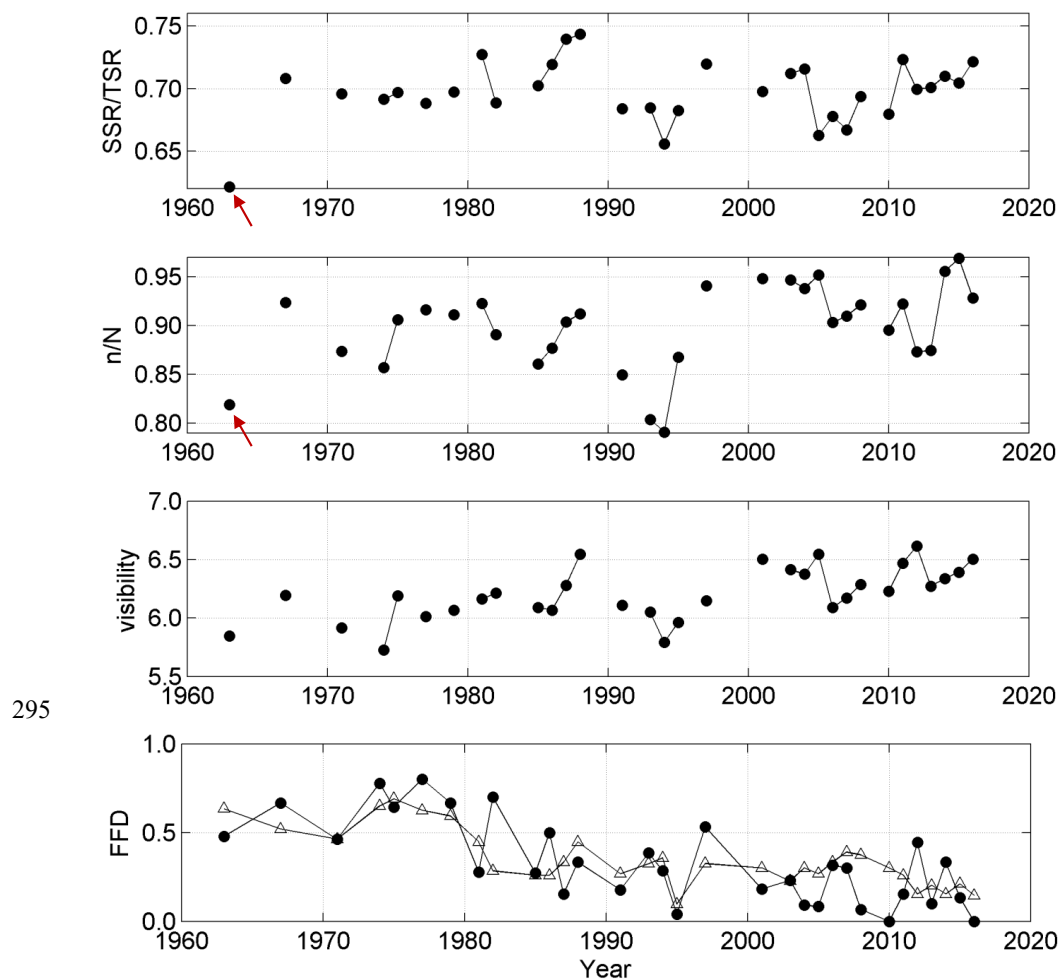
277 biomass burning plumes from long range transport can be detected in São Paulo
278 (Castanho and Artaxo, 2001, Landulfo et al., 2003, Freitas et al., 2005, Castanho et al.,
279 2008, Yamasoe et al., 2017). For these reasons, we restricted this analysis using data
280 from July to October only.

281 For the first period, the cloud free mean transmittance was 0.691 ± 0.029 and for
282 the second period, a mean value of 0.700 ± 0.023 was estimated. Applying the Student
283 t-test to compare the two means, we obtained $t = -0.87$ and $p = 0.40$, thus, the null
284 hypothesis cannot be rejected at the 95% significance level, indicating that under
285 cloudless sky the mean atmospheric transmittance over São Paulo was similar in both
286 periods, suggesting that changes in the aerosol direct effect were unlikely to explain the
287 distinct features observed in both periods. Nevertheless, from Figure 3, which illustrates
288 the mean atmospheric transmittance (SSR/TSR) in cloud free conditions (i. e., $SCF \leq$
289 0.1), in the first period, transmittance values were above 0.68, except in 1963, while in
290 the second period transmittance below 0.68 were more frequent, which might suggest
291 an increase in the atmospheric turbidity, particularly during the 1990's decade.
292 However, it is worth mention a recovery to higher transmittance values after 2010.
293 Similar features were also observed in n/N and horizontal visibility time series.

294



Long-Term Analysis of Surface Solar Radiation 16



295

296
297 Figure 3 – Mean variability of cloud-free (SCF ≤ 0.1) atmospheric transmittance
298 (SSR/TSR), normalized sunshine duration (n/N), horizontal visibility and fraction of
299 foggy days (FFD) from July to September in each year (open symbols) and on the
300 cloud-free days only in the same period (full symbols). The red arrow indicates the year
301 of volcano Agung eruption, in 1963, whose signal was detected in both SSR and SD
302 data. Only years with more than 9 cloud-free days were considered.

303

304

305 Figure 3 also shows that 1963 presented the lowest mean transmittance in the
306 series, and a decrease observed in the normalized sunshine duration series as well.



Long-Term Analysis of Surface Solar Radiation 17

307 According to Robertson et al. (2001), following Sato et al. (1993), one possible
308 explanation is the eruption of volcano Agung, whose plume affected southern latitudes,
309 with stratospheric AOD above 0.1 even one year after the eruption. Pinatubo eruption in
310 1991 also contributed to a high load of stratospheric AOD around latitude 25° S,
311 particularly one year after eruption, but no clear evidence was detected in our data.

312 Mean values of n/N varied from 0.841 ± 0.035 , in the first period, to
313 0.852 ± 0.047 , depicting a higher variability in the second one. Student t-test returned a
314 t value of -0.71, with $p = 0.49$, again indicating no difference in both periods. In
315 contrast, horizontal visibility mean value varied from 6.04 ± 0.17 to 6.27 ± 0.21 and the
316 Student t-test returned $t = -3.21$ and $p = 0.005$, indicating that horizontal visibility in the
317 second period was statistically higher than in the first period, at the 95% significance
318 level. Both n/N and horizontal visibility for cloudless sky presented an increasing trend
319 particularly after 2000 (Figure 3). A possible explanation for this behavior may be due
320 to a reduction over time in the frequency of haze, fog and mist. Notice that
321 transmittance is more sensitive to haze than n/N , since haze can last throughout the day,
322 affecting continuously the transmittance, while, for the conditions observed in São
323 Paulo, its efficiency to extinguish the direct solar beam is limited, therefore, yielding a
324 lower impact on sunshine duration measurements. According to Stanhill et al. (2014),
325 only when aerosol optical depth (AOD) exceeds 2 sunshine duration recorders can be
326 sensitive to aerosol loadings and only early in the morning and late in the afternoon
327 (Horseman et al., 2008). By contrast, fog exerts a significant effect on n/N , because its
328 strongest impact occurs early in the morning when it is more frequent and when mostly
329 of solar radiation is in the diffuse component. Moreover, the number of days with fog is
330 decreasing in São Paulo, and particularly on the analyzed cloud free days, the fraction of
331 foggy days (FFD) decreased throughout the years as illustrated in Figure 3, what can



Long-Term Analysis of Surface Solar Radiation 18

332 explain the increase of n/N in the recent years. This could also be the reason for the
333 positive trend of SD under all sky scenarios in the second period (Figure 2), when the
334 SFC increase was not significant. A decrease in the annual number of foggy days was
335 also observed in China (Li et al., 2012), which the authors attributed to the urban heat
336 island effect. As expected, horizontal visibility is also affected by the presence of fog,
337 although from Figure 3, only fog cannot explain all the variability observed in cloudless
338 sky conditions. During the late 1980's to early 1990's, transmittance, n/N and horizontal
339 visibility presented a significant decay clearly not related to the decrease observed in the
340 number of foggy days.

341 Concerning the urban heat island effect, the Metropolitan Area of São Paulo
342 experienced a fast growth rate from 1980 to 2010. There were nearly 12 million
343 inhabitants in 1980, and the population grew to about 21 million inhabitants in 2010
344 (Silva et al., 2017). According to the authors, the urban area increased from 874 km² to
345 2209 km², from 1962 to 2002. According to Kim and Baik (2002), the maximum UHI
346 intensity is more pronounced in clear sky conditions, occurs more frequently at night
347 than during the day, and decreases with increasing wind speed. However, Ferreira et al.
348 (2012) reported that, in São Paulo, the urban heat island maximum effect was observed
349 during day time, around 03:00 PM, and was associated with downward solar radiation
350 heating the urban region in a more effective way than the rural surrounding areas.

351 **3.3 Long term trends in daily maximum and minimum temperatures**

352 Figure 4 presents the temporal variation of the annual mean of the daily
353 maximum and minimum temperatures registered at the meteorological station, used to
354 estimate DTR. As discussed in the last paragraphs, if the increasing trend in SD over the
355 last years could be possibly attributed to the decreasing number of days per year with
356 fog occurrence, we now hypothesize on the possible reasons for the increasing trend of



Long-Term Analysis of Surface Solar Radiation 19

357 DTR in the second period. According to Dai et al. (1999), it should also respond to
358 cloud cover and precipitation and thus to SSR variations. As discussed by the authors,
359 clouds can reduce T_{\max} and increase T_{\min} , since they can reflect solar radiation back to
360 space and emit thermal radiation down to the surface, respectively. Such behaviors can
361 be clearly seen in Figure 4, in the first period, and confirmed by the trend analysis
362 presented in Table 3. During the dimming period, T_{\max} presented a negative trend, while
363 T_{\min} an increasing one, statistically significant at 95% confidence level for the last
364 variable. Similar behavior was observed by Wild et al. (2007) who argued that the
365 decreasing trend of T_{\max} is consistent with the negative trend of SSR, demonstrating that
366 solar radiation deficit at the surface presented a clear effect on the surface temperature.
367 Looking at the second period, from 1984 to 2016, both maximum and minimum
368 temperatures presented increasing trend, statistically significant at the 95% confidence
369 level, in the annual basis, of 0.25 °C per decade and 0.16 °C per decade, respectively. In
370 this period, T_{\min} trend was still in line with the increasing SFC trend, but as pointed out
371 by Wild et al. (2007) could also be a response to the increasing levels of greenhouse
372 gases as also pointed by de Abreu et al. (2019).

373

374 Table 3 - Modified Mann-Kendall trend test results for period 1, from 1961 to 1983, and
375 period 2, from 1984 to 2016, considering each season and in an annual basis, for the
376 daily maximum (T_{\max}) and minimum (T_{\min}) temperatures. The trend was estimated as
377 the slope of the linear fit between the variable of interest and year.

T_{\max}						
Period 1: 1961-1983				Period 2: 1984-2016		
Time interval	Trend	Z	p	Trend	Z	P
Annual	-0.11	-1.33	0.184	0.25	2.15	0.031
DJF	0.20	1.06	0.291	0.33	2.07	0.038

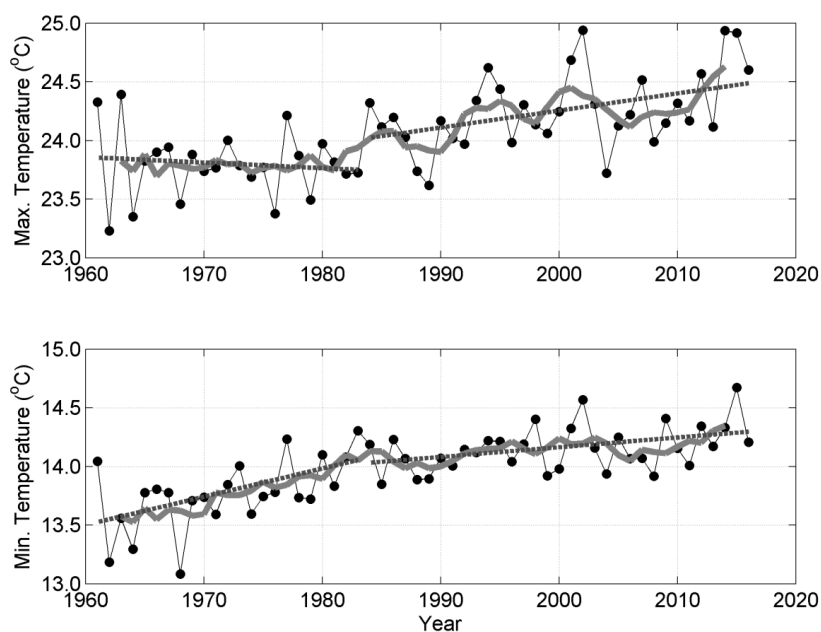


Long-Term Analysis of Surface Solar Radiation 20

MAM	-0.15	-0.79	0.430	0.03	0.23	0.816
JJA	0.02	0.26	0.795	0.33	2.68	0.007
SON	-0.26	-0.63	0.526	0.36	1.72	0.085
T_{min}						
Period 1: 1961-1983			Period 2: 1984-2016			
Time interval	Trend	Z	p	Trend	Z	P
Annual	0.56	2.54	0.011	0.16	2.15	0.031
DJF	0.53	2.96	0.003	0.13	2.68	0.007
MAM	0.52	2.71	0.007	-0.07	-0.79	0.429
JJA	0.62	1.58	0.113	0.26	1.78	0.075
SON	-0.03	0.63	0.526	0.26	2.43	0.015

378 Units of trend: °C per decade

379



380

381 Figure 4 - Annual mean variability of daily maximum and minimum air temperatures at
 382 1.5 meters. Gray curves represent 5 years moving averages and dotted lines are the
 383 result of trend analysis from 1961 to 1983 and from 1984 to 2016.

384



Long-Term Analysis of Surface Solar Radiation 21

385 From the previous discussion, although completely cloud free days were
386 extremely rare in São Paulo, the increase in T_{\max} in the second period can be attributed
387 to SSR changes associated with the aerosol direct effect only if the aerosol composition
388 changed from a more scattering to a more absorbing one, with a similar attenuation
389 effect on the solar radiation, as the atmospheric transmittance associated with aerosol
390 only was similar in both periods. A recent study by Andrade et al. (2017), discussing
391 changes over time in air quality conditions at the Metropolitan Area of São Paulo,
392 showed that SO_2 frequently exceeded the air quality standards in the 1980's. According
393 to the authors, the Brazilian government started a program to control its emission due to
394 the complaints of the population. At the beginning, the program focused on stationary
395 sources (industries) and, in the 1990's, the sulfur content in diesel fuel was also
396 targeted. Thus, as a consequence of this program, SO_2 concentrations declined and other
397 measures helped decreasing the concentration of particulate matter with diameter less
398 than $10\ \mu\text{m}$ (PM_{10}) near the surface. However, according to Oyama (2015), also due to a
399 political decision to stimulate the economy, the annual number of registrations of new
400 gasoline fueled vehicles increased exponentially, jumping from about 3000 vehicles in
401 1988, peaking in 2000 with 150000 registrations, decreasing slowly after that, to about
402 60000 in 2012.

403 Changes in aerosol chemical composition and consequently optical properties,
404 from more scattering to more absorbing, without affecting the atmospheric
405 transmissivity on cloud free days could possibly explain the effect on T_{\max} . Sulfate,
406 formed by gas to particle conversion of SO_2 , is efficient as cloud condensation nuclei
407 (Easter and Hobbs, 1974) and also presents high single scattering albedo (Takemura et
408 al. 2002). Even with the renovation of the vehicular fleet in São Paulo, old heavy duty
409 vehicles fueled with diesel still circulate in the MASP area, and according to Andrade et



Long-Term Analysis of Surface Solar Radiation 22

410 al. (2017) the diesel fleet constitute the main source of organic aerosols. In the case of
411 diesel fueled vehicles, the number of new registered vehicles in the São Paulo city
412 increased from about 5000 in 2000 to more than 25000 in 2010, the year with the
413 highest number of registrations (Oyama, 2015). According to Feng et al. (2019),
414 toluene secondary organic aerosol (SOA) presents low single scattering albedo in the
415 ultraviolet-visible spectral range (0.78 ± 0.02) and toluene is one of the most abundant
416 among the aromatic volatile hydrocarbons present in gasoline and other fuels (Brocco et
417 al, 1997, Yamamoto et al., 2000). Particles with high absorption efficiency to solar
418 radiation, such as black carbon, can cause heating of the atmosphere. According to
419 Martins et al. (2009) aerosol particles measured during the wintertime of 1999 (August
420 and September) presented high absorption efficiency in the ultraviolet spectrum, even
421 higher than black carbon, which the authors attributed to the organic aerosol component.
422 Previous results, from the AERONET (Aerosol Robotic Network) radiometer operating
423 in the city, reported relative low single scattering albedo for aerosols from local sources,
424 SSA at 550 nm around 0.85, (Castanho et al., 2008, Yamasoe et al., 2017).

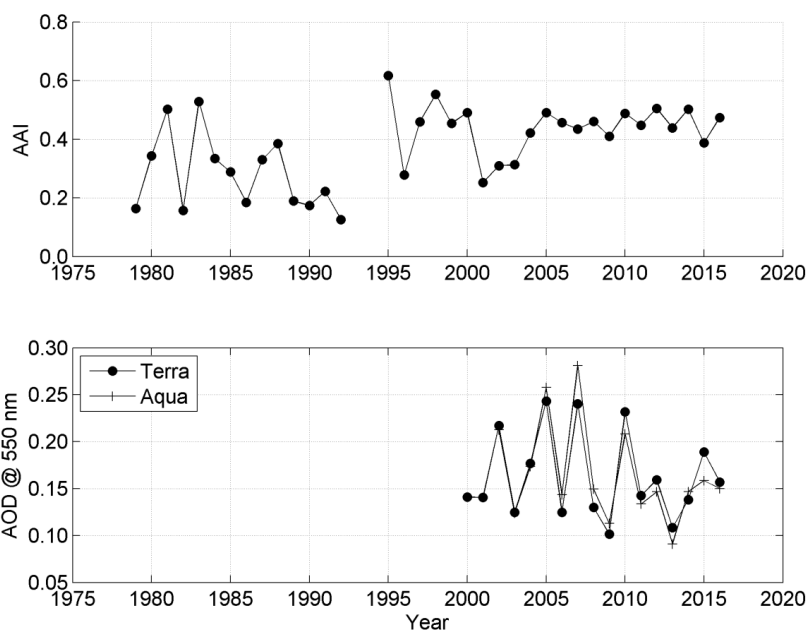
425 In order to verify the possibility of a pattern change in aerosol properties, from a
426 more scattering to a more absorbing one, without a significant change on aerosol
427 attenuation capacity, at least during the second period, annual mean values of absorbing
428 aerosol index and aerosol optical depth time series are presented in Figure 5. As
429 mentioned previously, data only for the months of July, August, September and October
430 were considered. For AAI, data are from 1979 to 2016 while for AOD, the MODIS in
431 2000 for Terra and 2002 for Aqua. Aerosol optical depth from MODIS onboard Terra
432 and Aqua satellites Figure 5 presents the annual mean values time series. From the
433 figure, annual mean AAI presented higher variability than mean AOD, particularly in
434 the 1980 and 1990 decades, varying from 0.1 to 0.6 in the period. AOD, by contrast,



Long-Term Analysis of Surface Solar Radiation 23

435 varied from 0.13 to 0.28. Now, in order to verify possible trends, considering the second
436 period only, i.e., from 1984 to 2016, the modified Mann-Kendall trend test was applied.
437 A statistically significant positive trend of 0.07 AAI per decade, at 95% confidence
438 level, was observed ($Z = 2.81$ and $p = 0.005$), consistent with the discussion from the
439 previous paragraph. Since satellite retrieval of aerosol optical depth over land started
440 only during the 2000's, no trend analysis was applied.

441



442

443 Figure 5 - Annual mean variability of absorbing aerosol index (AAI) (top) and aerosol
444 optical depth (AOD) from MODIS onboard Terra and Aqua satellites (bottom).

445

446 As discussed previously, due to the fast urbanization of the Metropolitan
447 Area of São Paulo (Silva et al., 2017), the urban heat island effect could also be
448 responsible to the observed increasing trend of T_{max} , particularly after 1980. Finally, as
449 pointed by Wild et al. (2007), the increasing atmospheric concentration of greenhouse



Long-Term Analysis of Surface Solar Radiation 24

450 gases (GHG) can be another reason for the observed trend of T_{\max} , which was masked
451 by the dimming effect in the first period. Modeling studies can help verify the real
452 causes and disentangle the contribution of each effect, which is, however, out of the
453 scope of this work.

454

455 **4 Conclusions**

456 This analysis of 56 years of surface solar irradiation (SSR) and proxies (SD and
457 DTR) data helped to show that from about 1960 to early 1980, named as first period, a
458 dimming effect of surface solar radiation was observed in the city of São Paulo,
459 consistent to other parts of the world. The positive trend of SCF in the first period
460 indicates that cloud variability could be one important driver of the dimming period.
461 The dimming effect was also confirmed by SD and DTR trends in the mentioned
462 period. However, the consistency between SSR, SD and DTR trends ended in 1983,
463 when SCF presented the highest value throughout the entire series and which coincided
464 with a strong El Niño year. Thus, answering our first question, SSR presented a
465 decreasing trend, throughout the 56 years of data, though not statistically significant at
466 the 95% confidence level in the first period, while it decreased at a rate of -0.41 kJ m^{-2}
467 per decade in the second one, from 1984 to 2016.

468 In the second period, the negative SSR trend was still consistent with the slight
469 positive trend of SCF, while the opposite behavior of SD and DTR indicated that other
470 factors besides the cloud cover variability might have affected their distinct patterns. In
471 order to understand the possible causes of the SD trends, a restrict analysis of alternative
472 parameters (fog frequency and horizontal visibility) focusing on cloud free days, for the
473 dry months of July to October, were analyzed, in spite of the limited number of
474 available days per year even allowing some flexibility ($\text{SCF} \leq 0.1$). The results



Long-Term Analysis of Surface Solar Radiation 25

475 indicated that the decreasing trend of the number of foggy days per year is a potential
476 candidate to explain part of the increasing trend of SD and horizontal visibility.
477 Although on cloud free days, no statistically significant difference was observed
478 between SD in the first and the second period. Only horizontal visibility on cloud free
479 days presented a statistically significant increase from the first to the second period. The
480 analysis of cloud free days also showed that the effect of Agung volcano eruption was
481 detected in both SSR and SD annual mean values. Due to Agung eruption, in 1963, the
482 annual mean transmittance was the lowest in the series. In the case of DTR, since it was
483 obtained from the difference between the daily maximum and minimum air
484 temperatures close to the surface, the trends of the annual mean values of these
485 temperatures were separately determined and analyzed. The T_{\min} positive trends
486 followed the SCF ones, with also possible influence of the increasing levels of
487 greenhouse gases, noticing that the decay observed in SCF, in the beginning of the
488 second period, is absent in the T_{\min} time series. The increasing trend of SCF, in the first
489 period, resulted in a decreasing trend in T_{\max} , as more solar radiation reaching the
490 surface was attenuated from year to year due to the presence of clouds. One hypothesis
491 for the increasing trend of T_{\max} during the second period was the changing of aerosol
492 optical properties in São Paulo, from a more scattering to a more absorbing one. Sulfate
493 particles, which scatter solar radiation with high efficiency, had the emission of
494 precursors to the atmosphere forced to decrease in the 1980's by governmental policies.
495 However, other political decisions, to promote economic development, caused the
496 increase of the gasoline fueled vehicles in São Paulo city in the beginning of the 1990's.
497 Gasoline and other fuels are important sources of toluene, whose SOA presents very
498 low single scattering albedo. The availability of an AERONET site in São Paulo, after
499 2000, made it possible to verify that the single scattering albedo of aerosol particles



Long-Term Analysis of Surface Solar Radiation 26

500 from local sources can be quite low. Data of absorbing aerosol index retrieved from
501 multiple satellites since 1979 and aerosol optical depth from MODIS onboard Terra and
502 Aqua satellites were analyzed to verify the hypothesis of changing aerosol optical
503 properties. The modified Mann-Kendall trend analysis for the AAI showed that this
504 variable presented a positive trend statistically significant at 95% confidence level
505 during the second period, although no trend analysis for AOD was performed because
506 of the short time series available. Other hypotheses are the urban heat island effect and
507 the increasing concentrations of GHG. Of course, changes in the wind pattern and
508 consequently in the advection of air masses with distinct properties can also affect the
509 air temperature locally.

510 As the resultant trends of SD and DTR, compared with the SSR trend, diverged
511 in the second period for São Paulo, in all sky conditions, caution might be taken when
512 those variables are used as proxies to downward surface solar radiation in the context of
513 dimming and brightening analyses. This study revealed that different factors may act on
514 each variable, leading to a distinct behavior, as also mentioned by Manara et al. (2017).

515 For future studies, modeling efforts may be able to help evaluate each hypothesis
516 raised in the present study, either those related to climate natural variability, such as El
517 Niño, or to those arising from anthropogenic activities as the increase of greenhouse gas
518 concentrations, land use changes, particularly through the imperviousness of soils,
519 affecting the partitioning of latent and sensible heat fluxes. Also, higher temporal
520 analysis and simultaneous monitoring of aerosol optical properties will help to better
521 evaluate the aerosol effects on downward solar radiation in this region, including via the
522 indirect effect.

523

524 **Data availability**



Long-Term Analysis of Surface Solar Radiation 27

525 Access to IAG meteorological station database (sky cover fraction, sunshine duration,
526 daily maximum and minimum air temperatures, number of foggy days, visibility and
527 irradiation data) for education or scientific use can be made under request at
528 http://www.estacao.iag.usp.br/sol_dados.php. The multi-sensor absorbing aerosol index
529 was downloaded from http://www.temis.nl/airpollution/absaai/#MS_AAI, while AOD
530 from MODIS on board Terra and Aqua satellites were obtained from
531 <https://giovanni.gsfc.nasa.gov/giovanni/>. All processed data used in the manuscript such
532 as annual and seasonal mean values, as well as data from cloud free days can be found
533 at <https://www.iag.usp.br/lraa/index.php/data/cientec/weather-station-climatology/>.

534

535 **Author contribution**

536 Conceptualization MAY and NMER; Methodology MAY; Data organization MAY and
537 SNSMA; Formal analysis MAY; Writing original draft MAY; Writing – Review &
538 Editing MAY, NMER, MW.

539

540 **Competing interest**

541 The authors declare that they have no conflict of interest.

542

543 **Acknowledgements**

544 The authors acknowledge Fundação de Amparo à Pesquisa do Estado de São Paulo
545 (FAPESP), grant number 2018/16048-6 and Coordenação de Aperfeiçoamento de
546 Pessoal de Nível Superior (CAPES) for financial support. Yamasoe acknowledges
547 CNPq (Conselho Nacional de Desenvolvimento Científico e Tecnológico), process



Long-Term Analysis of Surface Solar Radiation 28

548 number 313005/2018-4. This study is part of the Núcleo de Apoio à Pesquisa em
549 Mudanças Climáticas (INCLINE). The authors are grateful to the observers and staff of
550 the Instituto de Astronomia, Geofísica e Ciências Atmosféricas meteorological station
551 for making available the meteorological observations.

552

553 **References**

554 Andrade, M. F., Kumar, P., Freitas, E. D., Ynoue, R. Y., Martins, J., Martins, L. D.,
555 Nogueira, T., Perez-Martinez, P., Miranda, R. M., Albuquerque, T., Gonçalves, F. L. T.,
556 Oyama, B. and Zhang, Y. Air quality in the megacity of São Paulo: Evolution over the
557 last 30 years and future perspectives. *Atmospheric Environment* 159, 66-82, 2017.

558 Bristow, K. L. and Campbell, G. S. On the relationship between incoming solar
559 radiation and daily maximum and minimum temperature. *Agricultural and Forest*
560 *Meteorology* 31, 159-166, 1984.

561 Brocco, D., Fratarcangelli, R., Lepore, L., Petricca, M. and Ventrone, I. Determination
562 of aromatic hydrocarbons in urban air of Rome. *Atmospheric Environment* 31(4), 557-
563 566, 1997.

564 Castanho, A. D. A. and Artaxo, P. Wintertime and summertime São Paulo aerosol
565 source apportionment study. *Atmospheric Environment* 35, 4889-4902, 2001.

566 Castanho, A. D. de A., Martins, J. V. and Artaxo, P. MODIS aerosol optical depth
567 retrievals with high spatial resolution over an urban area using the critical reflectance. *J.*
568 *Geophys. Res.* 113, D02201, doi: 10.1029/2007JD008751, 2008.

569 Coelho, C. A. S., Firpo, M. A. F., Maia, A. H. N., and MacLachlan, C. Exploring the
570 feasibility of empirical, dynamical and combined probabilistic rainy season onset
571 forecasts for São Paulo, Brazil. *Int. J. Climatol.* 37 (Suppl. 1), 398-411, doi:
572 10.1002/joc.5010, 2017.

573 Dai, A., Trenberth, K. E. and Karl, T. R. Effects of clouds, soil moisture, precipitation,
574 and water vapor on diurnal temperature range. *Journal of Climate* 12, 2451-2473, 1999.

575 de Abreu, R. C., Tett, S. F. B., Schurer, A. and Rocha, H. R. Attribution of detected
576 temperature trends in Southeast Brazil. *Geophysical Research Letters*, 46, 8407-8414.
577 <https://doi.org/10.1029/2019GL083003>, 2019.

578 Dutton, E. G., Stone, R. S., Nelson, D. W. and Mendonca, B. G. Recent interannual
579 variations in solar radiation, cloudiness, and surface temperature at the South Pole.
580 *Journal of Climate* 4, 848-858, 1991.



Long-Term Analysis of Surface Solar Radiation 29

- 581 Easter, R. C. and Hobbs, P. V. The formation of sulfates and the enhancement of cloud
582 condensation nuclei in clouds. *Journal of the Atmospheric Sciences* 31, 1586-1594,
583 1974.
- 584 Feng, Z., Huang, M., Cai, S., Xu, X., Yang, Z., Zhao, W., Hu, C., Gu, X. and Zhang, W.
585 Characterization of single scattering albedo and chemical components of aged toluene
586 secondary organic aerosol. *Atmospheric Pollution Research* 10, 1736-1744. doi:
587 10.1016/j.apr.2019.07.005, 2019.
- 588 Ferreira, M. J., Oliveira, A. P., Soares, J., Codato, G., Bárbaro, E. W. and Escobedo, J.
589 F. Radiation balance at the surface in the city of São Paulo, Brazil: diurnal and seasonal
590 variations. *Theor. Appl. Climatol.* 107-229-246. doi: 10.1007/s00704-011-0480-2,
591 2012.
- 592 Freitas, S. R., K. M. Longo, M. A. F. S. Dias, P. L. S. Dias, R. Chatfield, E. Prins, P.
593 Artaxo, G. A. Grell, and F. S. Recuero. Monitoring the transport of biomass burning
594 emissions in South America, *Environ. Fluid Mech.*, 5, 135–167, 2005.
- 595 Graaf, M., Stammes, P., Torres, O., Koelemeijer, R. B. A. Absorbing Aerosol Index:
596 Sensitivity analysis, application to GOME and comparison with TOMS. *J. Geophys.*
597 *Res.* 110, D01201, doi: 10.1029/2004JD005178, 2005.
- 598 Hamed, K. H. and Rao, A. R. A modified Mann-Kendall trend test for autocorrelated
599 data. *Journal of Hydrology* 204, 182-196, 1998.
- 600 Herman, J. R., Barthia, P. K., Torres, O., Hsu, C., Seftor, C. and Celarier, E. A. Global
601 distributions of UV-absorbing aerosols from NIMBUS 7/TOMS data. *J. Geophys. Res.*
602 102(D14), 16911-16922, 1997.
- 603 Horseman, A., MacKenzie, A. R. and Timmis, R. Using bright sunshine at low-
604 elevation angles to compile an historical record of the effect of aerosol on incoming
605 solar radiation. *Atmos. Environ.* 42, 7600-7610, 2008.
- 606 Hsu, N. C., Tsay, S. C., King, M. D. and Herman, J. R. Aerosol properties over bright-
607 reflecting source regions. *IEEE Trans. Geosci. Remote Sens.*, 42, 557-569, 2004.
- 608 Kaufman, Y. J., Tanré, D., Remer, L., Vermote, E., Chu, A. Holben, B. N.
609 Operational remote sensing of tropospheric aerosol over land from EOS Moderate
610 Resolution Imaging Spectroradiometer. *J. Geophys. Res.* 102, 17051 – 17067, 1997.
- 611 Kim, Y.H. and Baik J. J. Maximum urban heat island intensity in Seoul. *J. Appl.*
612 *Meteorol.* 41, 651–659, 2002.
- 613 Kren, A. C., Pilewskie, P. and Coddington, O. Where does Earth’s atmosphere get its
614 energy? *J. Space Weather Space Clim.* 7(A10) doi: 10.1051/swsc/2017007, 2017.
- 615 Kumari, B. P. and Goswami, B. N. Seminal role of clouds on solar dimming over India
616 monsoon region. *Geophys. Res. Letters* 37 (L06703), 1-5, doi:10.1029/2009GL042133,
617 2010.
- 618 Landulfo, E., A. Papayannis, P. Artaxo, A. D. A. Castanho, A. Z. Freitas, R. F. Sousa,
619 N. D. Vieira Jr., M. P. M. P. Jorge, O. R. Sánchez-Ccoyllo, and D. S. Moreira.



Long-Term Analysis of Surface Solar Radiation 30

- 620 Synergetic measurements of aerosols over São Paulo, Brazil using LIDAR,
621 Sunphotometer and satellite data during the dry season, *Atmos. Chem. Phys.*, 3, 1523–
622 1539, 2003.
- 623 Li, Z., Yang, J., Shi, C. and Pu, M. Urbanization effects on fog in China: Field Research
624 and Modeling. *Pure Appl. Geophys.* 169, 927–939, doi: 10.1007/s00024-011-0356-5,
625 2012.
- 626 Makowski, K., Wild, M. and Ohmura, A. Diurnal temperature range over Europe
627 between 1950 and 2005. *Atmos. Chem. Phys.*, 8, 6483–6498, 2008.
- 628 Manara, V., Brunetti, M., Celozzi, A., Maugeri, M., Sanchez-Lorenzo, A. and Wild, M.
629 Detection of dimming/brightening in Italy from homogenized all-sky and clear-sky
630 surface solar radiation records and underlying causes (1959–2013). *Atmos. Chem. Phys.*
631 16, 11145–11161, doi:10.5194/acp-16-11145-2016, 2016.
- 632 Manara, V., Brunetti, M., Maugeri, M., Sanchez-Lorenzo, A. and Wild, M. Sunshine
633 duration and global radiation trends in Italy (1959–2013): To what extent do they agree?
634 *J. Geophys. Res. Atmos.* 122, 4312–4331, doi:10.1002/2016JD026374, 2017.
- 635 Martins, J. V., Artaxo, P., Kaufman, Y. J., Castanho, A. D. and Remer, L. A. Spectral
636 absorption properties of aerosol particles from 350–2500 nm. *Geophys. Res. Letters* 36,
637 L13810, doi: 10.1029/2009GL037435, 2009.
- 638 Obregón G. O., Marengo J. A. and Nobre C. A. Rainfall and climate variability: long-
639 term trends in the Metropolitan Area of São Paulo in the 20th century. *Clim Res* 61:93-
640 107. <https://doi.org/10.3354/cr01241>, 2014.
- 641 Ohvriil, H., Teral, R., Neiman, L., Kannel, M., Uustare, M., Tee, M., Russak, V.,
642 Okulov, O., Jõeveer, A., Kallis, A., Ohvriil, T., Terez, E. I., Terez, G. A., Gushchin, G.
643 K., Abakumova, G. M., Gorbarenko, E. V., Tsvetkov, A. V. and Laulainen, N. Global
644 dimming and brightening versus atmospheric column transparency, Europe, 1906–2007.
645 *J. Geophys. Res.* 114(D00D12), 1–17, doi:10.1029/2008JD010644, 2009.
- 646 Oyama, B. S. Contribution of the vehicular emission to the organic aerosol composition
647 in the city of São Paulo. (Doctoral Thesis). Universidade de São Paulo, São Paulo,
648 Brazil. Available at
649 https://www.iag.usp.br/pos/sites/default/files/t_beatriz_s_oyama_corrigida.pdf - last
650 access on October 25, 2019, 2015.
- 651 Paltridge, G. W. and Platt, C. M. R. Radiative processes in meteorology and
652 climatology. Elsevier Science, Amsterdam, Oxford, New York, 1976.
- 653 Plana-Fattori, A. and Ceballos, J. C. Algumas análises do comportamento de um
654 actinógrafo bimetálico Fuess modelo 58d. *Revista Brasileira de Meteorologia* 3 (2),
655 247–256, 1988.
- 656 Raichijk, C. Observed trends in sunshine duration over South America. *International*
657 *Journal of Climatology* 32, 669–680. Doi: 10.1002/joc.2296, 2012.



Long-Term Analysis of Surface Solar Radiation 31

- 658 Remer, L. A., Kaufman, Y. J., Tanre, D., Mattoo, S., Chu, D. A., Martins, J. V., Li, R.
659 R. , Ichoku, C., Levy, R. C., Kleidman, R. G., Eck, T. F., Vermote, E. and B. N.
660 Holben, B. N. The MODIS aerosol algorithm, products and validation. *J. Atmos. Sci.*,
661 62, 947-973, 2005.
- 662 Robertson, A., Overpeck, J., Rind, D., Mosley-Thompson, E., Zielinski, G., Lean, J.,
663 Koch, D., Penner, J., Tegen, I. and Healy, R. Hypothesized climate forcing time series
664 for the last 500 years. *J. Geophys. Res.* 106(D14), 14783-214803, 2001.
- 665 Rosas, J., Yamasoe, M. A., Sena E. T. and Rosário N. E. Cloud climatology from visual
666 observations at São Paulo, Brazil. *Int. J. Climatol.*, 1–13.
667 <https://doi.org/10.1002/joc.6203>, 2019.
- 668 Sato, M., Hansen, J. E., McCormick, M. P. and Pollack, J. B. Stratospheric aerosol
669 optical depths, 1850-1990. *J. Geophys. Res.* 98(D12), 22987-22994, 1993.
- 670 Sen, P. K. Estimates of the regression coefficient based on Kendall's Tau. *Journal of the*
671 *American Statistical Association* 63(324), 1379-1389, 1968.
- 672 Shi, G., Hayasaka, T., Ohmura, A., Chen, Z.-H., Wang, B., Zhao, J.-Q., Che, H.-Z. and
673 Xu, Li. Data quality assessment and the long-term trend of ground solar radiation in
674 China. *Journal of Applied Meteorology and Climatology* 47, 1006-1016, 2008.
- 675 Silva, F. B., Longo, K. M., and Andrade, F. M. Spatial and temporal variability patterns
676 of the urban heat island in São Paulo. *Environments* 4, 27, doi:
677 10.3390/environments4020027, 2017.
- 678 Stanhill, G. and Cohen, S. Global dimming: a review of the evidence for a widespread
679 and significant reduction in global radiation with discussion of its probable causes and
680 possible agricultural consequences. *Agricultural and Forest Meteorology* 107, 255-278,
681 2001.
- 682 Stanhill, G., Achiman, O., Rosa, R. and Cohen, S. The cause of solar dimming and
683 brightening at the Earth's surface during the last half century: Evidence from
684 measurements of sunshine duration. *J. Geophys. Res. Atmos.* 119, 10902-10911.
685 doi:10.1002/2013JD021308, 2014).
- 686 Takemura, T., Nakajima, T., Dubovik, O., Holben, B. N. and Kinne, S. Single-
687 scattering albedo and radiative forcing of various aerosol species with a global three-
688 dimensional model. *Journal of Climate* 15(4), 333-352, 2002.
- 689 Tilstra, L. G., Graaf, M., Tuinder, O. N. E., van der A, R. J., and Stammes, P.
690 Monitoring aerosol presence over a 15-year period using the Absorbing Aerosol Index
691 measured by GOME-1, SCIAMACHY, and GOME-2, *Proceedings of the ESA Living*
692 *Planet Symposium 2013, ESA Special Publication SP-722*, 2014.
- 693 Torres, O., Barthia, P. K., Herman, J. R., Ahmad, Z. and Gleason, J. Derivation of
694 aerosol properties from satellite measurements of backscattered ultraviolet radiation:
695 Theoretical basis. *J. Geophys. Res.* 103(D14), 17099-17110, 1998.



Long-Term Analysis of Surface Solar Radiation 32

- 696 Xavier, T. M. B. S., Silva Dias, M. A. F. and Xavier, A. F. S. Impact of ENSO episodes
697 on the autumn rainfall patterns near São Paulo, Brazil. *Int. J. Climatol.* 15. 571-584,
698 1995.
- 699 Wild, M., Gilgen, H., Roesch, A., Ohmura, A., Long, C. N., Dutton, E. G., Forgan, B.,
700 Kallis, A., Russak, V., and Tsvetkov, A. From dimming to brightening: decadal changes
701 in solar radiation at Earth's surface. *Science* 308, 847-850, 2005.
- 702 Wild, M., Ohmura, A., and Makowski, K. Impact of global dimming and brightening on
703 global warming. *Geophys. Res. Lett.* 34, L04702, doi: 10.1029/2006GL028031, 2007.
- 704 Wild, M. Global dimming and brightening: A review. *J. Geophys. Res.* 114(D00D16),
705 doi: 10.1029/2008JD011470, 2009.
- 706 Wild, M. Enlightening global dimming and brightening. *BAMS* 93, 27-37,
707 doi:10.1175/BAMS-D-11-00074.1, 2012.
- 708 Wild, M., Folini, D., Schär, C., Loeb, N., Dutton, E. G. and König-Langlo, G. The
709 global energy balance from a surface perspective. *Clim. Dyn.* 40, 3107-3134, doi:
710 10.1007/s00382-012-1569-8, 2013.
- 711 Wild, M. Towards global estimates of the surface energy budget. *Curr. Clim. Change*
712 *Rep.* 3, 87-97. doi: 10.1007/s40641-017-0058-x, 2017.
- 713 Yamamoto, N., Okayasu, H., Murayama, S., Mori, S., Hunahashi, K. and Suzuki.
714 Measurement of volatile organic compounds in the urban atmosphere of Yokohama,
715 Japan, by an automated gas chromatographic system. *Atmospheric Environment* 34,
716 4441-4446, 2000.
- 717 Yamasoe, M. A., N. M. E. do Rosário, and K. M. Barros. Downward solar global
718 irradiance at the surface in São Paulo city—The climatological effects of aerosol and
719 clouds, *J. Geophys. Res. Atmos.*, 122, 391–404, doi:10.1002/2016JD025585, 2017.